ACS OMEGA

Open Access

http://pubs.acs.org/journal/acsodf

Article

In Situ Polymerization Electrospinning of Amine−Epoxy/Poly(vinyl alcohol) Nanofiber Webs for Direct CO_2 Capture from the Air

Chisato Okada,* Zongzi Hou, Hiroaki Imoto, Kensuke Naka, Takeshi Kikutani, and Midori Takasaki

Cite This: *ACS Omega* 2024, 9, 50466−50475

Read Online

ACCESS | Metrics & More | Article Recommendations

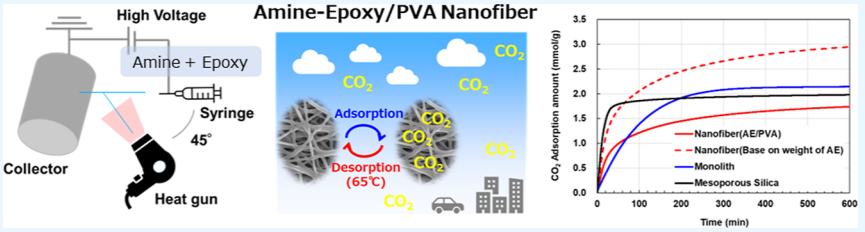

ABSTRACT: To achieve carbon neutrality by 2050, there is a growing need to actively capture carbon dioxide (CO_2) from the atmosphere. As a method to capture CO_2 directly from the atmosphere, direct air capture (DAC) is attracting attention and amine-based compounds have been extensively studied as CO_2 adsorbents. In this research, we developed thermosetting DAC nanofibers with excellent low-temperature desorption properties and good heat resistance by polymerizing an amine with epoxy. For the fabrication of epoxy-cross-linked amine nanofibers through the electrospinning process, poly(vinyl alcohol) (PVA) was added for the improvement of spinnability, and the direct spin-line heating was conducted for the in situ thermal polymerization. As a result, nanofiber webs with fiber diameters of approximately 300−400 nm were fabricated successfully. The investigation of the CO_2 adsorption and desorption performance of the obtained amine/epoxy/PVA (AE/PVA) nanofiber webs verified the high adsorption amount of 1.8 mmol/g at a CO_2 concentration of 400 ppm. Additionally, 93% of adsorbed CO_2 could be desorbed at a low temperature of 65 °C. These results suggested the possibility of low-energy-consumption CO_2 recovery. By improving the adsorption rate and by making desorption possible at low temperatures, the adsorption/desorption cycle can be repeated more quickly, increasing the amount of CO_2 that can be recovered in a day. The prepared webs also exhibited an excellent adsorption retention ratio of 75% after 100 h of operation at 85 °C, while general amine-filled mesoporous silica usually shows a retention ratio of only 13%. In addition, FT-IR, DSC, and elemental analysis of amine/epoxy/PVA nanofibers were carried out to analyze the reaction mechanism during fiber production. It was revealed that PVA was not involved in the reaction, and as in the bulk state, almost all primary amines were converted to secondary amines due to the in situ polymerization of amines and epoxy to form nanofibers.

1. INTRODUCTION

There are various gases that cause global warming, but carbon dioxide is said to be the gas that has the greatest impact on global warming.[1−3] Carbon dioxide (CO_2) emissions have been continuing to increase due to our extensive use of fossil fuels such as oil, coal, and natural gas since the beginning of the Industrial Revolution.[4] Exhaust gas from thermal power plants and factories contains large amounts of CO_2. For nearly 20 years, CO_2 has been recovered from those high-concentration gases using the amine absorption method to reduce carbon emissions.[5] However, to achieve carbon neutrality in 2050, it is essential not only to suppress carbon dioxide emissions but also to capture the CO_2 already released into the atmosphere. For example, low CO_2 concentration gases emitted from cars, airplanes, and exhaled air are released into the atmosphere. Therefore, direct air capture (DAC) is attracting attention as a technology for directly capturing CO_2 released into the atmosphere from the past to the present. Utilizing the DAC technology, CO_2, which is extremely dilute at 400 ppm in the atmosphere, is adsorbed onto an adsorbent and then recovered by heating or pressure reduction.[6−8] After the capturing of CO_2, in the carbon capture and storage (CCS) technology, CO_2 is stored underground at a high concentration of over 99%; therefore, high concentration capturing is essential in the DAC technology.

The DAC technologies can be categorized into (1) chemical adsorption methods, (2) physical adsorption methods, (3)

Received: August 18, 2024
Revised: November 21, 2024
Accepted: November 25, 2024
Published: December 11, 2024

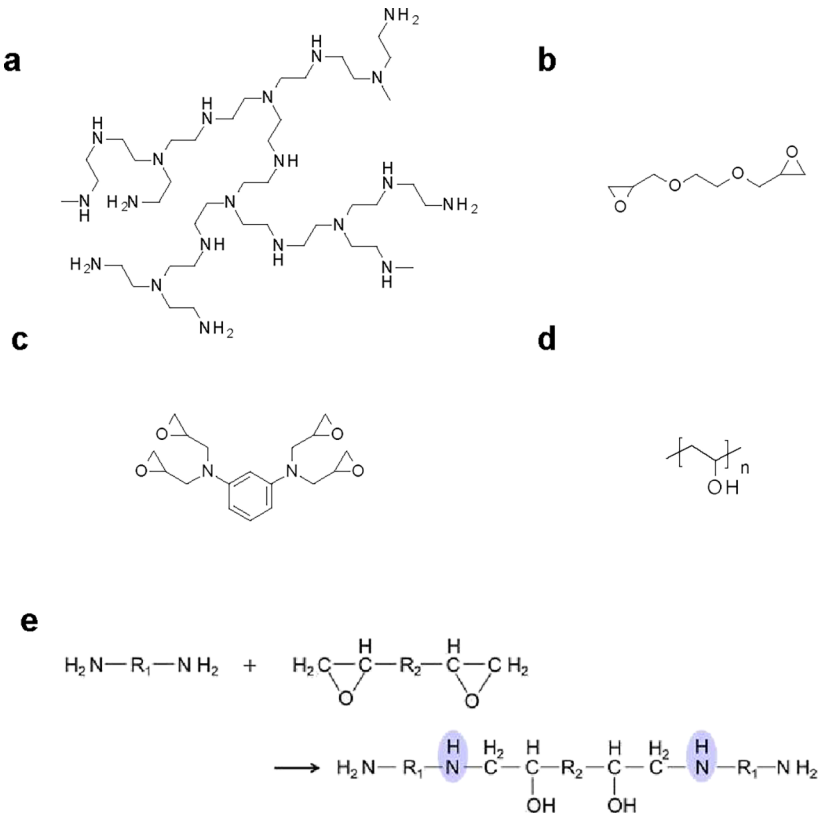

Figure 1. Chemical structural formula of (a) PEI, (b) EDE, (c) T-X, and (d) PVA and (e) chemical reaction of amine and epoxy to form secondary amine as indicated.

membrane separation methods, and (4) cryogenic separation methods. The chemical adsorption methods include the technology using liquid amines[9] or alkaline aqueous solutions, that use amino acids,[10] and the one using alkali metal salts,[11] amine-supported porous materials,[12] metal organic frameworks,[13−15] and ion exchange resins.[16] The chemical adsorption method is a technology that selectively adsorbs CO_2 into an adsorption liquid by bringing an amine or alkaline aqueous solution into contact with a gas containing CO_2 and then heats the adsorption liquid to separate and recover highly pure CO_2. Although this technology is suitable for separating and recovering highly concentrated or large amounts of CO_2, it requires a large amount of energy and is not cost-effective for recovering low-concentration CO_2.[17,18]

The physical adsorption method simply utilizing porous materials such as zeolite[17] and activated carbon is not realistic because of the low amount of adsorption.[19−21]

The membrane separation method uses polymer membranes[22] or ionic liquid membranes,[23] with a separation function to enable continuous separation and recovery. Unlike other chemical adsorption methods and physical adsorption methods, there is no energy consumption, such as heating and depressurization. Therefore, it is said to be energy-efficient; however, it is difficult to increase the carbon dioxide concentration after recovery.

Cryogenic separation is a method of recovering gas by compressing, cooling, and separating it using the difference in the boiling point of gases. In this process, CO_2 is cooled into dry ice.[24] However, compared with other separation methods, the capital investment cost and the energy required for recovery are high. Due to the large size of the plant, the technology has not been put into practical use.

Currently, the most promising approach to practical application is chemical adsorption with a large specific surface area, which involves coating a porous material such as mesoporous silica with liquid amine.[12] By filling such porous material, the liquid amine can be handled like a solid. However, it has problems such as volatilization of amine at high temperatures, poor heat resistance, and leakage in the presence of water. This is because liquid amine generally has low molecular weight and contains abundant primary amines,[25,26] which are also susceptible to deterioration such as oxidation reactions. It is also known that the energy efficiency of primary amine is low because it requires a high desorption temperature, even though it has extremely high reactivity and easily adsorbs CO_2.

It is generally known that by cross-linking amines with materials such as epoxy and polymerizing them, it is possible to impart heat resistance by suppressing volatilization at high temperatures and to prevent outflow due to moisture, thereby improving handling. However, the disadvantage of polymerizing primary amines is that the number of CO_2 adsorption sites is reduced, the amount of adsorption is decreased, and the adsorption rate is reduced.[27]

For suppressing the decrease in adsorption rate by increasing the specific surface area while improving handling and heat resistance, the conversion of polymerized amines into nanofibers is considered to be a promising method. There have been various reports on the fabrication of fibers for CO_2 adsorption, such as amino silane-grafted zirconia/titania/silica-poly(amide-imide) (PAI) composite hollow fiber,[28] PAI hollow fiber filled with porous silica supported with polyethylenimine (PEI),[29−31] porous silica fiber loaded with PEI,[32] and L-arginine nanofiber.[33] Nevertheless, there are

https://doi.org/10.1021/acsomega.4c07631
ACS Omega 2024, 9, 50466−50475

concerns that these CO_2 adsorption fibers have a low adsorption amount due to low amine density and that their heat resistance is low due to the large amount of primary amines that remain.

In this research, we were conscious of the carbon footprint of products (CFP) when producing solid adsorbents and aimed for an environmentally friendly manufacturing method using a water-based system. However, the production of nanofibers using thermosetting resins such as epoxy has not been studied much.

Within the limit of our knowledge, in the past, only fibers with diameters of a few micrometers or more were obtained from epoxy resins or blends of epoxy resins. For example, carbon fiber-reinforced epoxy and montmorillonite nanoclay nanocomposite,[34] cross-linked basic immobilized amine sorbent within a porous cellulose acetate fiber,[35] epoxy fiber with the diameter of 3 μm by electrospinning,[36] epoxy/poly caprolactone fiber with a shape memory effect,[37] and epoxy nanofiber from the core of core/shell fiber[38] were reported. On the other hand, PEI was reacted with epoxy only after its fiber formation to prepare practically applicable heavy metal ion absorbent fibers.[39] That is because epoxy is a curable resin with irreversible reactions. These methods require multiple manufacturing steps and provide only fibers of a large diameter.

In this study, we attempted to fabricate amine epoxy/poly(vinyl alcohol) (PVA) (AE/PVA) fibers of fine diameters by in situ heating polymerization during the electrospinning process. The main purpose was to convert thermally unstable primary amines into secondary amines by reacting with epoxy and then to create nanofibers with a high specific surface area.

2. EXPERIMENTAL SECTION

2.1. Materials. The chemical structure of the material used to manufacture the nanofibers is shown in Figure 1. PEI (purity 98−100%, SP-006, Nippon Shokubai Co., Ltd., Tokyo, Japan) was used as an amine, and the mixture of ethylene glycol diglycidyl ether (EDE) (purity >99%, EX-810, Nagase ChemteX Corporation, Osaka, Japan) and *N,N,N′,N′*-tetraglycidyl-*m*-xylenediamine (T-X) (purity >98%, TETRAD-X, Mitsubishi Gas Chemical Co., Inc., Tokyo, Japan) was used as an epoxy. It is known that the thermal resistance of amine can be improved by heating the mixture of amine and epoxy at around 60 °C, where the conversion of primary amine to secondary amine through the reaction with epoxy and the solidification through the cross-linking proceeds. As shown in Figure 1e, in the cross-linking reaction, all thermally unstable primary amines can be eliminated through the conversion to secondary amines by mixing with the chemical equivalent of epoxy e.q./primary amine e.q. = 0.5. The EDE and T-X mixing ratio of 8:2 was adopted to control the glass transition temperature to be around 20 °C. It should be noted that the glass transition temperature of adsorbents is supposed to be close to the adsorption temperature in the operation of DAC for optimum adsorption and desorption performance.

The typical chemical structure of PEI is shown in Figure 1a. The PEI used in this research has a molecular weight of 600, an amine value of 20 mmol/g, and a molar ratio of primary, secondary, and tertiary amines obtained through the NMR analysis of 35:35:30. The primary amine equivalent in the PEI of 142.86 g/mol was estimated from the amine value and the composition of primary amine, while the epoxy equivalents for EDE and T-X are 87.1 g/mol and 99.0 g/mol, respectively. Accordingly, to realize an epoxy e.q./primary amine e.q. of 0.5, the mixing ratio of PEI/(EDE/T-X) of 8:(4:1) in weight ratio, which corresponds to 5.32:(9.20:1) in molar ratio, was adopted. The chemical reaction of amine and epoxy to form a secondary amine is also indicated in Figure 1e.

In addition, to introduce the spinnability to the spinning dope, the prepared amine/epoxy mixture was mixed with the PVA water solution. First, the PVA/water 7 wt % solution was prepared by dissolving PVA (purity >93%, molecular weight 75,000, hydrolysis 99%, Kuraray Co., Tokyo, Japan) into the water at 95 °C for 2 h. Subsequently, the spinning dope was prepared by mixing the PVA/water solution and the amine/epoxy mixture with a weight ratio of 9:1, which corresponds to the PEI:(EDA:T-X):PVA solution of 8:(4:1):117 in weight ratio, and 5.32:(9.20:1):0.04 in molar ratio.

2.2. Electrospinning Equipment. Electrospinning was conducted using an electrospinning apparatus (NEU, Kato Tech, Kyoto, Japan) equipped with a stationary cylindrical collector. First, after filling the prepared amine/epoxy solution into a 5 mL syringe with a 22 G needle, electrospinning was conducted with an extrusion rate of 0.46 mL/h, nozzle−collector distance of 100 mm, and applied voltage of 10 kV. For the acceleration of polymerization in the spinning process, the collector was heated to 100 °C in some experiments. For another type of attempt to accelerate the polymerization, a heat gun was introduced into the process to heat the spinning path between the needle and collector. The direction of the air blow was set at an angle of 45° to the axis connecting the needle and the collector. The setting temperature of the heat gun was changed from 70 to 160 °C. A constant air speed of 3.48 m/s measured using a differential pressure-type air velocimeter (testo400, Testo SE & Co KGaA., Titisee-Neustadt, Germany) was adopted. The influence of the heat gun on the surface temperature of the collector was minimal; at the heat gun setting temperature of 160 °C, the collector surface temperature was 47 °C. The prepared fiber web was dried in a vacuum oven (VOS-310C, EYELA, Tokyo, Japan) at 60 °C for 2 h before the adsorption/desorption test.

2.3. Analysis of the Prepared Web. *2.3.1. Scanning Electron Microscopy.* The prepared web was observed using a scanning electron microscope (SU-3800, HITACHI High-Tech Co., Tokyo, Japan) with a magnification of 3000 and 10,000×. Mean fiber diameter was obtained from the obtained image data using image analysis software (ImageJ).

2.3.2. Differential Scanning Calorimetry. The chemical reaction of the amine/epoxy mixture (A + E), amine/epoxy/PVA (A + E + PVA) mixture, and PVA was analyzed through measurement of the heat of the chemical reaction using a differential scanning calorimeter (DSC2500, TA Instruments, Newcastle, DE, USA). The measurement was conducted under a nitrogen atmosphere with the first heating, cooling, and second heating cycles in the temperature range from −50 to 175 °C. The heating and cooling rate was 10 °C/min, and the holding time at the highest temperature was 1 min. The second heating cycle was used to confirm the disappearance of the heat caused by the residual chemical reaction. Furthermore, the glass transition temperature of the prepared web was analyzed with the same temperature program. In this case, the first heating was conducted to evaporate the absorbed water.

2.3.3. Infrared Absorption Analysis. Progress of the chemical reaction was traced through the analysis of the variation of the functional group using an FT-IR spectroscope

https://doi.org/10.1021/acsomega.4c07631
ACS Omega 2024, 9, 50466−50475

(Nicolet iS5, FT-IR, Thermo Fisher Scientific Inc., Waltham, MA, USA).

2.3.4. Elemental Analysis. Elemental analysis of the prepared web was conducted by using a CHN elemental analyzer (varioEL III, Elementar, Langenselbold, Germany) equipped with a thermal conductivity detector. Measurement conditions were with a combustion tube temperature of 950 °C, reduction tube temperature of 500 °C, and carrier gas of He (200 mL/min). The oxygen concentration was obtained by subtracting the total of the C, H, and N elemental compositions from 100%.

2.4. Adsorption/Desorption Test. A schematic of the adsorption and desorption measurement systems is shown in Figure 2. It consists of a 10% CO_2/N_2 gas cylinder, a N_2 gas

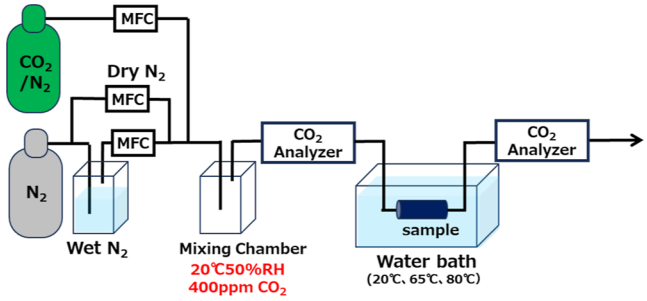

Figure 2. Schematic of the adsorption/desorption measurement system.

cylinder, a N_2 gas humidifier, a gas mixing chamber, mass flow controllers, gas analyzers for measurement of the CO_2 concentration, a sample tube, and a water bath. The dry N_2 gas supplied from the cylinder was partially humidified by bubbling and mixed with 10% CO_2/N_2 dry gas. The flow rate of each gas was adjusted with a mass flow controller and mixed in the mixing chamber to obtain a flow with a CO_2 concentration of 400 ppm, temperature of 20 °C, relative humidity of 50%, and flow rate of 300 mL/min.

The web sample was vacuum-dried at 60 °C for 2 h before the adsorption test. The CO_2/N_2 mixture gas with 400 ppm of CO_2, which corresponds to the recent atmospheric CO_2 concentration on the earth, was introduced to a sample tube filled with 50 mg of sample. First, the sample tube was immersed in 80 °C hot water for the desorption of CO_2 and subsequently immersed in 20 °C water for 1000 min. The CO_2 concentration of the inlet and outlet gas was continuously analyzed using a CO_2 analyzer (LI-850, MEIWAFOSIS, Tokyo, Japan). The amount of adsorption was obtained by integrating the CO_2 concentration difference between the inlet and outlet gases throughout the experiment. The desorption amount was analyzed similarly by monitoring the difference in the CO_2 concentration after immersing the test tube in 65 °C water. The desorption ratio was evaluated based on the desorption amount at 65 °C for 90 min. The adsorption test was also applied to the samples after the heat treatment at 85 °C for 100 h to evaluate the thermal resistance.

2.5. Amine Efficiency. The CO_2−amine reactions under dry and humid conditions are shown in Figure 3. The CO_2−amine reaction under dry conditions requires one CO_2 molecule and two primary or secondary amine moieties to give a carbamate (reaction A or B). Thus, the maximum CO_2/N ratio achievable by chemical reaction with amine sorbents under such conditions is 0.5 (0.5 mol of CO_2 per 1.0 mol of N). The molar CO_2/N ratio is defined as the amine efficiency. When moisture is present, a reaction yielding carbonate or bicarbonate (depending on the pH) can be observed (reaction C). As seen from these reactions, the maximum achievable CO_2/N ratio under humid conditions is 1.0 (1.0 mol of CO_2 per 1.0 mol of N), double that of the corresponding anhydrous conditions.[19]

3. RESULTS AND DISCUSSION

3.1. Spinning Behavior. First, the nanofiber formation was attempted using a mixture of amine and two types of epoxies as shown in Figure 1 and applying the electrospinning apparatus shown in Figure 2a. Spinning conditions were as follows: gauge of injection needle 22 G, needle to collector distance 10 cm, throughput 0.46 mL/h, and room temperature. Even though the applied voltage varied widely from 8 to 20 kV, the stock solution merely dripped from the tip of the syringe, and fiber formation was impossible. This was thought to be because of the mixture being insufficiently charged.

Second, a spinning dope was prepared by mixing the 7 wt % PVA aqueous solution with the amine/epoxy mixture to impart spinnability. The reason for the selection of PVA for the improvement of spinnability of AE was that PVA is a water-soluble polymer, which is a merit from the viewpoint of CFP. It was found through the preliminary test that other water-soluble polymers such as poly(vinylpyrrolidone) and poly(acrylic acid) were not suitable for this application.

Under the same spinning conditions as the amine/epoxy mixture and an applied voltage of 10 kV, the dope was charged, and the spinning jet reached the collector. However, fibers were not formed, and a sticky transparent nonporous membrane was obtained as shown in Figure 5a. On the other hand, spinning of a simple aqueous solution of 7 wt % PVA was possible, and fine fibers with a diameter of 200 nm could be obtained as shown in Figure 5b. Although the formation of fibers in the spinning process of the amine/epoxy/PVA mixture was possible, the amine and epoxy monomers did not polymerize, and the spinning dope remained in a liquid state after reaching the collector and merely spread on the collector surface. Therefore, the collector was heated to a surface temperature of 100 °C to promote the polymerization of the amine and epoxy monomers, and the spinning was carried out under the same conditions as in Figure 4a. The obtained fiber is shown in Figure 5c. From the scanning electron microscopy (SEM) images, fibers with a

$$2\text{R-NH}_2 + \text{CO}_2 \leftrightarrow \text{R-NH}_3^+ + \text{R-NH-COO}^- \quad \text{(A)}$$

$$2\text{R}_1\text{R}_2\text{-NH} + \text{CO}_2 \leftrightarrow \text{R}_1\text{R}_2\text{-NH}_2^+ + \text{R}_1\text{R}_2\text{-NH-COO}^- \quad \text{(B)}$$

$$\text{R}_1\text{R}_2\text{-NH} + \text{CO}_2 + \text{H}_2\text{O} \leftrightarrow \text{R}_1\text{R}_2\text{-NH}_2^+\text{HCO}_3^- \leftrightarrow \text{R}_1\text{R}_2\text{-NH}_2^+\text{CO}_3^{2-} \quad \text{(C)}$$

Figure 3. CO_2-amine reactions under dry and humid conditions. (a) Reaction of CO_2−primary amine under dry condition, (b) reaction of CO_2−secondary amine under dry condition, and (c) reaction of CO_2−primary and secondary amine under humid condition.

https://doi.org/10.1021/acsomega.4c07631
ACS Omega 2024, 9, 50466−50475

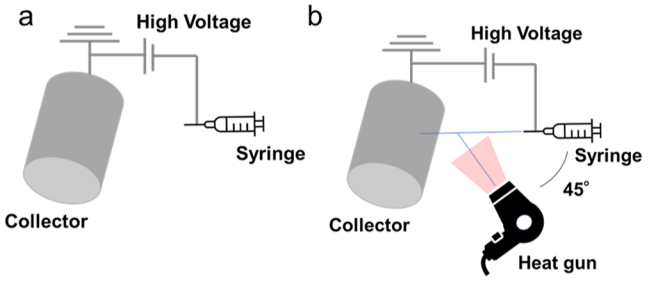

Figure 4. Process schematic for making fibers by electrospinning; (a) without heating and (b) heating with a heat gun.

diameter of approximately 2−5 μm were formed at the early stage of deposition through the promotion of polymerization; however, a nonporous membrane similar to that shown in Figure 5a was obtained after further deposition of fibers because of the insufficient polymerization.

Therefore, heating the spinning path between the needle and collector was attempted to accelerate the polymerization of the amine and epoxy monomers before deposition on the collector by introducing hot air blowing using a heat gun. More concretely, the direction of air blow was adjusted to 45° to the axis connecting the needle and collector, the setting temperature of the heat gun was varied from 70 to 160 °C, and a constant air speed of 3.48 m/s was adopted. For each set temperature condition of the heat gun, the air temperature in the area where the fiber was jetting is shown in Table 1. Even when the temperature of the heat gun was set at 160 °C, the surface temperature of the collector was approximately 47 °C, confirming that the heating of the fibers in space by the heat gun did not have a large effect on the collector temperature.

It was confirmed that nanofibers were formed on the collector by using the in situ heating spinning method. Table 1 also shows the SEM images of the webs obtained by changing the temperature of the heat gun and the average fiber diameter measured from the SEM images. Fibers were not obtained at room temperature, and a nonporous membrane was formed. When the heat gun temperature was 70 °C, it was possible to observe the fiber shape. Although the obtained web was not sticky, it could be seen that the fibers adhered to each other at contact points such as intersections. At 80 °C, no adhesion was observed between the fibers, and a fiber web with an average fiber diameter of 300 nm could be produced. Even when the temperature was further increased, a fiber web similar to that at 80 °C was obtained. However, the higher the temperature, the thicker the fibers became, reaching over 400 nm at 140 °C.

In general, the viscosity decreases at high temperatures, but at the same time, an increase in the solvent evaporation rate and an increase in the polymerization reaction rate lead to an increase in viscosity. It is thought that the final diameter in electrospinning is determined by the temperature dependence of these competing effects, and under the conditions of this experiment, it is thought that the effect of increasing the evaporation rate or polymerization rate was exceeded, and the fiber diameter increased with the increase in temperature.

The differential scanning calorimetry (DSC) thermogram of the web prepared with a heat gun temperature of 120 °C is shown in Figure 6. The endothermic peak was observed in the first heating because of the vaporization of water, whereas no distinct peak was observed in the second heating. Figure 6b is the enlarged curve of the second heating. The glass transition was clearly observed at 9.31 °C, which was close to the targeted Tg of around 20 °C.

3.2. Adsorption/Desorption Test. Figure 7 and Table 2 show the CO_2 adsorption/desorption test results for the AE/PVA nanofiber web prepared at 120 °C. The results for monolith (amine/epoxy monolith, sponge-like porous media)[40] and mesoporous silica with a PEI surface coating,[40] which were previously prepared in our group, are shown for comparison. The adsorption amount and adsorption half-time in Table 2 were evaluated based on the CO_2 adsorption at 1000 min, whereas the desorption ratio was obtained from the amount of desorption after 90 min at 65 °C.

The adsorption speed of AE/PVA nanofibers was faster than that of the monolith with the same amine/epoxy composition, as shown in Figure 7. The adsorption half-time, i.e., the time required to reach half of the saturated adsorption amount, for the nanofiber web was approximately 39 min. This was significantly shorter compared to 68 min for the monolith. The dotted line in the figure indicates the variation of the amount of adsorption evaluated excluding the mass of PVA. The saturated adsorption amount after 1000 min for the AE/PVA nanofibers of 1.8 mmol/g was lower in comparison with that for the monolith of 2.1 mmol/g; however, the adsorption amount of the nanofibers evaluated excluding the mass of PVA, which does not participate in the adsorption amount, is 3.05 mmol/g. This indicates the higher amine efficiency of the nanofiber in comparison with the monolith.

In summary, the nanofiber showed faster adsorption as well as a higher amine efficiency in comparison to the monolith. The adsorption speed of silica with an adsorption half-time of 11 min was faster in comparison with the nanofiber and monolith; however, the thermal resistance of silica is known to be low because of the existence of the primary amine, which will be discussed later.

It should be noted that the desorption speed is generally much faster than the adsorption speed and almost completes within a few minutes. The amount of desorption evaluated through the desorption ratio after 90 min at 65 °C was higher

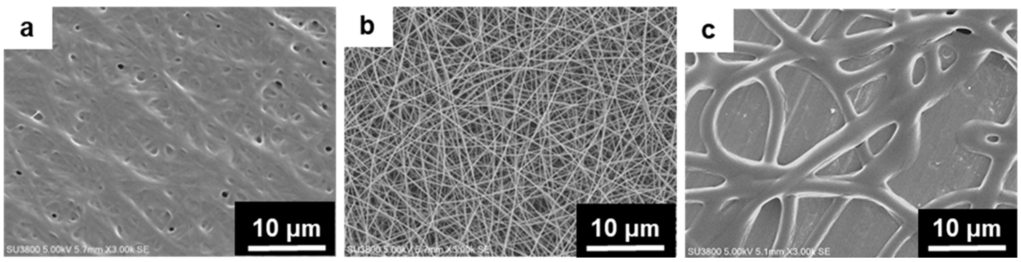

Figure 5. SEM images of the top surface of electrospun sheet/fiber; (a) amine−epoxy/PVA prepared at room temperature, (b) only PVA prepared at room temperature, and (c) amine−epoxy/PVA prepared at 100 °C (collector temperature).

https://doi.org/10.1021/acsomega.4c07631
ACS Omega 2024, 9, 50466−50475

Table 1. Heat Gun Set Temperature, Ambient Air Temperature, Average Fiber Diameter, and SEM Images with 3000 and 10,000× Magnifications for Electrospun AE/PVA

Set temp (℃)	No heating	70	80	90	100	120	140	160
Air temp (℃)	–	54	65	76	82	102	119	137
Diameter (nm)	–	Inter-connected	317	361	362	395	413	419
SEM Image (×3k)	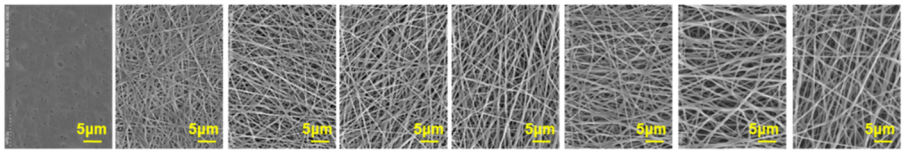							
SEM Image (×10k)	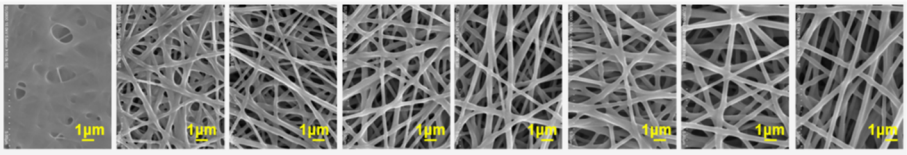							

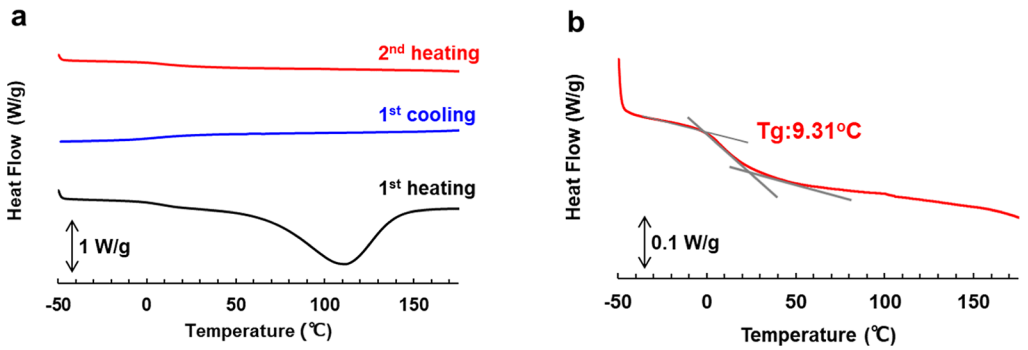

Figure 6. DSC thermograms measured with a heating and cooling rate of 10 °C/min for the AE/PVA nanofiber web prepared with a heat gun temperature of 120 °C; (a) DSC curves during heating, cooling, and second heating cycles, and (b) enlarged DSC curve of the second heating.

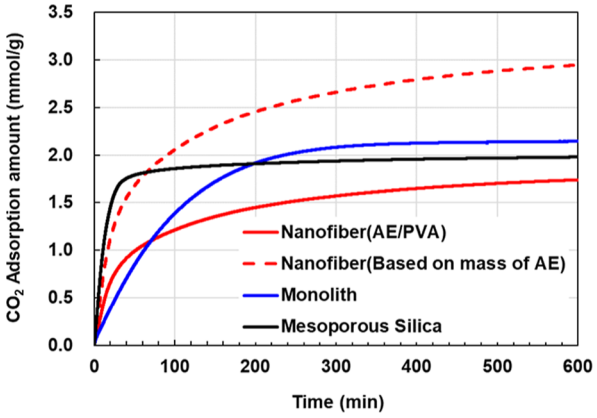

Figure 7. Variation of CO_2 adsorption amount with time measured at 20 °C, 50%RH using the N_2 mixture gas with a CO_2 content of 400 ppm for the AE/PVA nanofiber web, and the corresponding data calculated excluding the mass of PVA (based on mass of AE). Data for amine−epoxy monolith and mesoporous silica filled with liquid amine are also shown for comparison.[40]

Table 2. Results of the CO_2 Adsorption and Desorption Test for the AE/PVA Nanofiber Web Prepared with a Heat Gun Temperature of 120 °C[a]

	nanofiber	monolith	mesoporous silica
adsorption amount (mmol/g)	1.8	2.1	2.0
adsorption half-time (min)	39	68	11
desorption ratio after 90 min at 65 °C (%)	93	97	83
amine efficiency (%)	23	20	27
heat resistance (%)	75	76	13

[a]Data for amine−epoxy monolith and mesoporous silica are also shown for comparison.[40]

than 90%, high enough for applying this material to the DAC system.

The heat resistance of the samples was investigated by comparing the adsorption amount before and after the heat treatment at 85 °C for 100 h, as shown in Figure 8. Retentions of adsorption were higher than 75% for the nanofiber and monolith. These values are sufficiently high for the application. On the other hand, even though silica showed higher adsorption amounts, its heat resistance was much lower mainly because of the primary amine in the structure. In addition, the molecular weight of amine on the silica is considered to be low. This means there is a possibility of the vaporization of amine during the heat treatment.

In summary, it was confirmed that nanofibers have higher performance than monoliths. However, the morphology of nanostructures between monoliths and nanofibers is markedly different, and the relationship between the specific surface area, for example, and the adsorption characteristics, which are

https://doi.org/10.1021/acsomega.4c07631
ACS Omega 2024, 9, 50466−50475

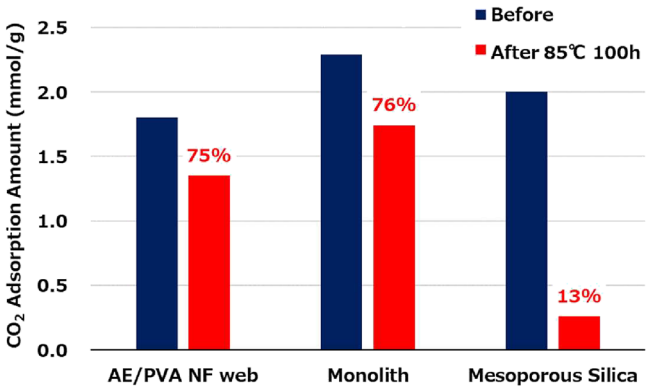

Figure 8. Saturated adsorption amount of CO_2, before and after 100 h of heat treatment at 85 °C for the AE/PVA nanofiber web. Data for amine−epoxy monolith and mesoporous silica filled with liquid amine are shown for comparison. Retention ratios representing heat resistance properties are also indicated.

considered to be closely related, needs to be examined in more detail.

3.3. Mechanism of Amine Epoxy Fiber Formation. It was confirmed that the formation of amine/epoxy fibers containing PVA is possible by electrospinning the mixture with a heat gun. Therefore, the fiber formation mechanism of this system, which involves chemical reactions, was investigated through DSC, FT-IR, and elemental analyses.

3.3.1. Analysis of Heat Reaction. The heat of the reaction for the amine/epoxy mixture with and without PVA (AE and AE + PVA) was analyzed by applying DSC. The results are summarized in Figure 9 and Table 3. The reaction between amine and epoxy is exothermic, starting at approximately 40 °C and exhibiting a peak at 90 °C. The thermograms for the AE and AE + PVA were similar, and there was no exothermic reaction for the pure PVA sample. The exothermic heat corresponding to the amount of AE was 422.1 and 424.5 J/g,

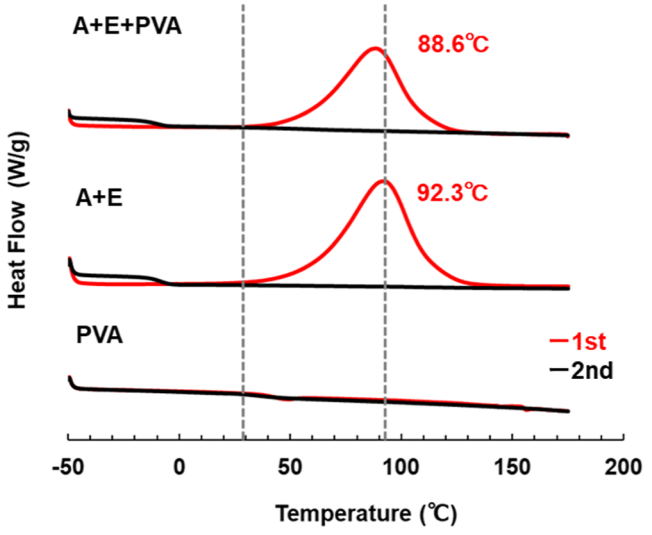

Figure 9. DSC curves of the first and second heating for the analysis of the heat of reaction (HR) measured at the heating rate of 10 °C/min for the mixture of amine, epoxy, and PVA (A + E + PVA), the mixture of amine and epoxy (A + E), and pure PVA. Peak temperatures HR for (A + E + PVA) and (A + E) are shown in the figure.

Table 3. Results of the Heat of Reaction (HR) Analysis from DSC Measurement for the Mixture of Amine, Epoxy, and PVA (A + E + PVA), the Mixture of Amine and Epoxy (A + E), and Pure PVA

	sample mass (mg)	AE mass (mg)	peak temp (°C)	HR per sample mass (J/g)	HR per mass of A and E (J/g)	mass fraction
A + E + PVA	7.52	5.59	88.6	315.4	424.5	AE 74.3%
A + E	4.09	4.09	92.3	422.1	422.1	
PVA	7.28					

and the peak temperatures were 92.3 and 88.6 °C for the AE and AE + PVA, respectively, indicating that PVA was not involved in the chemical reaction of amine and epoxy. There was a slight acceleration of the reaction of amine and epoxy, which was considered to be due to the presence of the hydroxyl group of PVA.

3.3.2. Analysis of Chemical Reaction. The results of FT-IR measurement for a mixture of amine monomer and epoxy monomer (A + E), amine−epoxy polymer (AE), PVA, and a mixture of AE and PVA (AE + PVA) are shown in Figure 10.

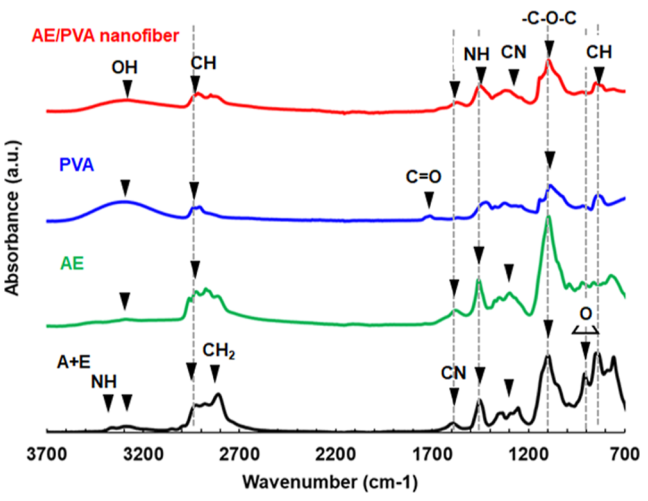

Figure 10. ATR-FTIR spectra of the AE/PVA nanofiber, pure PVA, the reaction product of amine and epoxy (AE), and the mixture of amine and epoxy (A + E).

First, the sample was dried in a vacuum oven of 60 °C for the desorption of CO_2. The measurement was conducted in a dry environment at room temperature with a dew point of −60 °C. For A + E, the peaks at 750 and 3400 cm^{-1} can be assigned to the NH bending vibration from the primary amine and the stretching vibration of the primary and secondary amines, respectively. The peak at 910 cm^{-1} corresponds to the antisymmetric stretching of the epoxy ring, which is characteristic of epoxy monomers, while the peak at 1600 cm^{-1} is for the C═C stretching vibration of the benzene ring in one of the epoxy components, TETEAD-X. After the chemical reaction of amine and epoxy (AE), the peak from the epoxy group at 910 cm^{-1} disappeared, and an already existing peak at around 1100 cm^{-1}, which also corresponds to the stretching vibration of newly formed −C−O−, became stronger. Furthermore, due to the formation of OH, a broad peak at 3300 cm^{-1}, which can be assigned to the stretching vibration of OH, appeared. It should be noted that the disappearance of N−H bending vibration

https://doi.org/10.1021/acsomega.4c07631
ACS Omega 2024, 9, 50466−50475

from the primary amine at 750 cm^{-1} and the intensity increase of N−H bending vibration from the secondary amine near 1580 cm^{-1} indicate that the primary amine selectively reacted with the epoxy. On the other hand, PVA exhibited peaks at 1087 cm^{-1} for the C−O stretching vibration, at 3300 cm^{-1} for the OH stretching vibration, and at 1711 cm^{-1} for the C═O stretching vibration for the remaining acetate group after the saponification. The FT-IR spectrum for AE + PVA was a simple mixture of spectra for AE and PVA, indicating that the PVA did not disturb the chemical reaction of amine and epoxy, and also, there was no chemical reaction between either PVA and amine nor PVA and epoxy.

3.3.3. Elemental Analysis. Because electrospinning was performed while heating, elemental analysis of the obtained nanofibers was performed to verify whether the monomers were volatilized during the spinning. The results of elemental analysis are shown in Table 4. For PEI, the measured values and theoretical values based on published chemical structures are shown. For a mixture of the amine and epoxy reactants and PVA (AE + PVA), the measured values of a film prepared from a varnish solution of (AE + PVA) through casting and curing at 100 °C and electrospun nanofibers as well as the theoretical values estimated from its chemical structure and composition are shown. For PEI, the measured and theoretical values of C, H, and N were almost identical except for the emergence of a slight oxygen fraction, which seems to be the effect of oxidation and/or adsorption of moisture. The (AE + PVA) originally contains oxygen due to the presence of PVA, while the theoretical values and the measured values are in good agreement except for a slight increase in the oxygen fraction. In addition, when comparing films and nanofibers with different manufacturing methods, the oxygen fraction was slightly higher for nanofibers that were subjected to a higher temperature during the process. Nevertheless, the theoretical and measured values were generally in good agreement, and it was judged that amines and epoxy monomers were not volatilized in the production of films and nanofibers.

Table 4. Result of the Elemental Analysis for PEI, AE/PVA Cast Film, and AE/PVA Nanofiber[a]

	C (wt %)	H (wt %)	N (wt %)	O (wt %)
PEI	53.5	11.7	32.2	2.6
PEI theoretical value	55.8	11.6	32.6	0.0
AE/PVA film	53.1	9.5	12.4	25.0
AE/PVA nanofiber	50.9	9.5	11.8	27.7
AE + PVA theoretical value	55.7	9.8	12.2	22.3

[a]Theoretical values estimated from the chemical structure for PEI and AE + PVA are also shown.

4. CONCLUSIONS

The AE/PVA nanofibers were successfully fabricated by using in situ polymerization electrospinning. By heating the space between the needle and collector above the reaction temperature of the epoxy, AE/PVA nanofibers of approximately 300 to 400 nm diameter were obtained. The obtained AE/PVA nanofiber web adsorbed 1.8 mmol/g of CO_2 from the N_2 mixture gas with a CO_2 content of 400 ppm and desorbed 93% of CO_2 by heating to 65 °C. Furthermore, it showed high heat resistance with a retention rate of saturated adsorption amount of 75% after heat treatment at 85 °C for 100 h. It was also inferred through FT-IR, DSC, and elemental analysis of amine/epoxy/PVA nanofibers that the same reaction as in the bulk state occurred in the in situ polymerized nanofibers. The process developed in this research is superior in easily producing thermosetting resin nanofibers without using solvents, and it can be said that it is possible to manufacture CO_2 adsorbents with low environmental load.

AUTHOR INFORMATION

Corresponding Author

Chisato Okada − *Nitto Denko Corporation, Osaka 567-8680, Japan; Faculty of Molecular Chemistry and Engineering, Kyoto Institute of Technology, Kyoto Institute of Technology, Sakyo-ku, Kyoto 606-8585, Japan;* orcid.org/0009-0004-2900-4432; Email: chisato.okada@nitto.com

Authors

Zongzi Hou − *Faculty of Materials Science and Engineering, Kyoto Institute of Technology, Sakyo-ku, Kyoto 606-8585, Japan;* Present Address: China Textile Academy, Beijing 100025, China

Hiroaki Imoto − *Faculty of Molecular Chemistry and Engineering, Kyoto Institute of Technology, Kyoto Institute of Technology, Sakyo-ku, Kyoto 606-8585, Japan;* orcid.org/0000-0003-1495-3059

Kensuke Naka − *Faculty of Molecular Chemistry and Engineering, Kyoto Institute of Technology, Kyoto Institute of Technology, Sakyo-ku, Kyoto 606-8585, Japan;* orcid.org/0000-0002-4516-6296

Takeshi Kikutani − *Institute of New Industry Incubation, Institute of Science Tokyo, Yokohama, Kanagawa 226-8503, Japan;* orcid.org/0000-0003-2644-3064

Midori Takasaki − *Faculty of Materials Science and Engineering, Kyoto Institute of Technology, Sakyo-ku, Kyoto 606-8585, Japan;* Present Address: Division of Artificial Environment and Information Research, Graduate School of Environment and Information Sciences, Yokohama National University, 79−7 Tokiwadai, Hodogaya-ku, Yokohama 240−8501, Japan.

Complete contact information is available at: https://pubs.acs.org/10.1021/acsomega.4c07631

Author Contributions

CRediT: Chisato Okada: conceptualization, formal analysis, investigation, methodology, resources, supervision, validation, visualization, and writing—review and editing; Zongzi Hou: supervision, visualization, and writing—review and editing; Hiroaki Imoto: supervision, visualization, and writing—review and editing; Kensuke Naka: supervision, visualization, and writing—review and editing; Takeshi Kikutani: conceptualization, formal analysis, investigation, methodology, resources, supervision, validation, visualization, and writing—review and editing; Midori Takasaki: conceptualization, formal analysis, investigation, methodology, resources, supervision, validation, visualization, and writing—review and editing.

Notes

The authors declare no competing financial interest.

ACKNOWLEDGMENTS

We wish to thank Nitto Denko Corporation for their significant support. I'm so thankful to have a supportive colleague. Finally, we are grateful to the referees for useful comments.

https://doi.org/10.1021/acsomega.4c07631
ACS Omega 2024, 9, 50466−50475

REFERENCES

(1) Stocker, T. F.; Qin, D.; Plattner, G.-K.; Tignor, M.; Allen, S. K.; Boschung, J.; Nauels, A.; Xia, Y.; Bex, V.; Midgley, P. M. *IPCC, 2013: Climate Change 2013: The Physical Science Basis. Contribution of Working Group I to the Fifth Assessment Report of the Intergovernmental Panel on Climate Change*; Cambridge University Press: Cambridge, United Kingdom and New York, NY, USA, 2013, p 1535.

(2) Lenssen, N. J. L.; Schmidt, G. A.; Hansen, J. E.; Menne, M. J.; Persin, A.; Ruedy, R.; Zyss, D. Improvements in the GISTEMP uncertainty model. *J. Geophys. Res. Atmos.* **2019**, *124*, 6307−6326.

(3) Breyer, C.; Fasihi, M.; Bajamundi, C.; Creutzig, F. Direct Air Capture of CO_2: A Key Technology for Ambitious Climate Change Mitigation. *Joule* **2019**, *3*, 2053−2065.

(4) Board, O. S. E. National Academies of Sciences, and Medicine. *Negative Emissions Technologies and Reliable Sequestration: A Research Agenda*; National Academies Press: Washington, DC, 2019.

(5) Kenarsari, S. D.; Yang, D. L.; Jiang, G. D.; Zhang, S. J.; Wang, J. J.; Russell, A. G.; Wei, Q.; Fan, M. H. Review of recent advances in carbon dioxide separation and capture. *RSC Adv.* **2013**, *3*, 22739−22773.

(6) McQueen, N.; Gomes, K. V.; McCormick, C.; Blumanthal, K.; Pisciotta, M.; Wilcox, J. A review of direct air capture (DAC): scaling up commercial technologies and innovating for the future. *Prog. Energy.* **2021**, *3*, 032001.

(7) Bisotti, F.; Hoff, K.; Mathisen, A.; Hovland, J. Direct Air capture (DAC) deployment: A review of the industrial deployment. *Chem. Eng. Sci.* **2024**, *283*, 119416.

(8) Shi, X.; Xiao, H.; Azarabadi, H.; Song, J.; Wu, X.; Chen, X.; Lackner, K. S. Sorbents for the Direct Capture of CO_2 from Ambient Air. *Angew. Chem., Int. Ed.* **2020**, *59*, 6984−7006.

(9) Rochelle, G. T. Amine Scrubbing for CO_2 Capture. *Science* **2009**, *325*, 1652−1654.

(10) Hussain, M. A.; Soujanya, Y.; Sastry, G. N. Evaluating the efficacy of amino acids as CO_2 capturing agents: a first principles investigation. *Environ. Sci. Technol.* **2011**, *45*, 8582−8588.

(11) Stolaroff, J. K.; Keith, D. W.; Lowry, G. V. Carbon Dioxide Capture from Atmospheric Air Using Sodium Hydroxide Spray. *Environ. Sci. Technol.* **2008**, *42* (8), 2728−2735.

(12) Jung, H.; Jo, D. H.; Lee, C. H.; Chung, W.; Shin, D.; Kim, S. H. Carbon Dioxide Capture Using Poly(ethylenimine)-Impregnated Poly(methyl methacrylate)-Supported Sorbents. *Energy Fuels* **2014**, *28* (6), 3994−4001.

(13) Ding, M.; Flaig, R. W.; Jiang, H.-L.; Yaghi, O. M. Carbon capture and conversion using metal−organic frameworks and MOF-based materials. *Chem. Soc. Rev.* **2019**, *48*, 2783−2828.

(14) Mcdonald, T. M.; Lee, W. R.; Mason, J. A.; Wiers, B. M.; Hong, C. S.; Long, J. R. Capture of Carbon Dioxide from Air and Flue Gas in the Alkylamine-Appended Metal−Organic Framework mmen-Mg2-(dobpdc). *J. Am. Chem. Soc.* **2012**, *134*, 7056−7065.

(15) Darunte, L. A.; Oetomo, A. D.; Walton, K. S.; Sholl, D. S.; Jones, C. W. Direct Air Capture of CO2 Using Amine Functionalized MIL-101(Cr). *ACS Sustainable Chem. Eng.* **2016**, *4* (10), 5761−5768.

(16) Alesi, W. R., Jr.; Kitchin, J. R. Evaluation of a Primary Amine-Functionalized Ion-Exchange Resin for CO2 Capture. *Ind. Eng. Chem. Res.* **2012**, *51* (19), 6907−6915.

(17) Samanta, A.; Zhao, A.; Shimizu, G. K.; Sarkar, P.; Gupta, R. Post-Combustion CO2 Capture Using Solid Sorbents: A Review. *Ind. Eng. Chem. Res.* **2012**, *51* (4), 1438−1463.

(18) Goto, K.; Yogo, K.; Higashii, T. A review of efficiency penalty in a coal-fired power plant with post-combustion CO2 capture. *Appl. Energy* **2013**, *111*, 710−720.

(19) Sanz-Pérez, E. S.; Murdock, C. R.; Didas, S. A.; Jones, C. W. Direct Capture of CO_2 from Ambient Air. *Chem. Rev.* **2016**, *116*, 11840−11867.

(20) Varcoe, J. R.; Atanassov, P.; Dekel, D. R.; Herring, A. M.; Hickner, M. A.; Kohl, P. A.; Kucernak, A. R.; Mustain, W. E.; Nijmeijer, K.; Scott, K.; Xu, T.; Zhuang, L. Anion-exchange membranes in electrochemical energy systems. *Energy Environ. Sci.* **2014**, *7*, 3135−3191.

(21) Kumar, A.; Madden, D. G.; Lusi, M.; Chen, K.-J.; Daniels, E. A.; Curtin, T.; Perry, J. J., IV; Zaworotko, M. J. Direct Air Capture of CO_2 by Physisorbent Materials. *Angew. Chem., Int. Ed.* **2015**, *54*, 14372−14377.

(22) Brunetti, A.; Scura, F.; Barbieri, G.; Drioli, E. Membrane technologies for CO_2 separation. *J. Membr. Sci.* **2010**, *359* (359), 115−125.

(23) Zeng, S.; Zhang, X.; Bai, L.; Zhang, X.; Wang, H.; Wang, J.; Bao, D.; Li, M.; Liu, X.; Zhang, S. Ionic-Liquid-Based CO_2 Capture Systems: Structure, Interaction and Process. *Chem. Rev.* **2017**, *117* (14), 9625−9673.

(24) Song, C.; Kitamura, Y.; Jiang, W. Application of Free Piston Stirling Cooler (SC) on CO_2 Capture Process. *Energy Procedia* **2013**, *37*, 1239−1245.

(25) Zoannou, K.-S.; Sapsford, D. J.; Griffiths, A. J. Thermal degradation of monoethanolamine and its effect on CO2 capture capacity. *Int. J. Greenhouse Gas Control* **2013**, *17*, 423−430.

(26) Lepaumier, H.; Picq, D.; Carrette, P.-L. New Amines for CO2 Capture. I. Mechanisms of Amine Degradation in the Presence of CO2. *Ind. Eng. Chem. Res.* **2009**, *48* (20), 9061−9067.

(27) Elfving, J.; Bajamundi, C.; Kauppinen, J. Characterization and Performance of Direct Air Capture Sorbent. *Energy Procedia* **2017**, *114*, 6087−6101.

(28) Brennan, P. J.; Thakkar, H.; Li, X.; Rownaghi, A. A.; Koros, W. J.; Rezaei, F. Effect of Post-Functionalization Conditions on the Carbon Dioxide Adsorption Properties of Aminosilane-Grafted Zirconia/Titania/Silica-Poly(amide-imide) Composite Hollow Fiber Sorbents. *Energy Technol.* **2017**, *5* (2), 327−337.

(29) Fan, Y.; Kalyanaraman, J.; Labreche, Y.; Rezaei, F.; Lively, R. P.; Realff, M. J.; Koros, W. J.; Jones, C. W.; Kawajiri, Y. CO_2 Sorption Performance of Composite Polymer/Aminosilica Hollow Fiber Sorbents: An Experimental and Modeling Study. *Ind. Eng. Chem. Res.* **2015**, *54*, 1783.

(30) Labreche, Y.; Fan, Y.; Rezaei, F.; Lively, R. P.; Jones, C. W.; Koros, W. J. Poly(amide-imide)/Silica Supported PEI Hollow Fiber Sorbents for Postcombustion CO2 Capture by RTSA. *ACS Appl. Mater. Interfaces* **2014**, *6* (21), 19336−19346.

(31) Li, F. S.; Labreche, Y.; Lively, R. P.; Lee, J. S.; Jones, C. W.; Koros, W. J. Poly(ethyleneimine) infused and functionalized Torlon®-silica hollow fiber sorbents for post-combustion CO_2 capture. *Polymer* **2014**, *55*, 1341.

(32) Gebald, C.; Wurzbacher, J. A.; Tingaut, P.; Zimmermann, T.; Steinfeld, A. Amine-based nanofibrillated cellulose as adsorbent for CO_2 capture from air. *Environ. Sci. Technol.* **2011**, *45* (20), 9101−9108.

(33) Korah, M. M.; Ly, S.; Barbosa, T. S.; Nile, R.; Jin, K.; Lackner, K. S.; Green, M. D. Electrospun Poly(vinyl alcohol)−l-Arginine Nanofiber Composites for Direct Air Capture of CO2. *ACS ES&T Engg.* **2023**, *3* (3), 373−386.

(34) Xu, Y.; Ho, S. V. Mechanical properties of carbon fiber reinforced epoxy/clay nanocomposites. *Compos. Sci. Technol.* **2008**, *68*, 854−886.

(35) Wilfong, W. C.; Wang, Q.; Ji, T.; Baker, J. S.; Shi, F.; Yi, S.; Gray, M. L. Directly Spun Epoxy-Crosslinked Polyethylenimine Fiber Sorbents for Direct Air Capture and Postcombustion Capture of CO_2. *Energy Technol.* **2022**, *10*, 2200356.

(36) Shneider, M.; Sui, X. M.; Greenfeld, I.; Wagner, H. D. Electrospinning of epoxy fibers. *Polymer* **2021**, *235*, 124307.

(37) Iregui, A.; Irusta, L.; Llorente, O.; Martin, L.; Calvo-correas, T.; Eceiza, A.; González, A. Electrospinning of cationically polymerized epoxy/polycaprolactone blends to obtain shape memory fibers (SMF). *Eur. Polym. J.* **2017**, *94*, 376−383.

(38) Wang, X.; Zhang, W.-J.; Yu, D.-G.; Li, X.-Y.; Yang, H. Epoxy resin nanofibers prepared using electrospun core/sheath nanofibers as templates. *Macromol. Mater. Eng.* **2013**, *298*, 664−669.

(39) Wang, X.; Min, M.; Liu, Z.; Yang, Y.; Zhou, Z.; Zhu, M.; Chen, Y.; Hsiao, B. S. Poly(ethyleneimine) nanofibrous affinity membrane fabricated via one step wet-electrospinning from poly(vinyl alcohol)-

https://doi.org/10.1021/acsomega.4c07631
ACS Omega 2024, 9, 50466−50475

doped poly(ethyleneimine) solution system and its application. *J. Membr. Sci.* **2011**, *379*, 191−199.
(40) Matsuda, K. Acid Gas Adsorption and Desorption Material. U.S. Patent US 0,001,336, 2024 .

https://doi.org/10.1021/acsomega.4c07631
ACS Omega 2024, 9, 50466−50475